Chemical oxidation of ibuprofen in the presence of iron species at near neutral pH

N. Sabri [a], K. Hanna [b], V. Yargeau [a],*

[a] Department of Chemical Engineering, McGill University, 3610 University Street, Montreal, Quebec, Canada H3A2B2
[b] Ecole Nationale Supérieure de Chimie de Rennes, UMR CNRS 6226 "Sciences Chimiques de Rennes" Avenue du Général Leclerc, 35708 Rennes, France

ARTICLE INFO

ABSTRACT

The objective of this work was to evaluate the removal of ibuprofen (IBP) using the oxidants hydrogen peroxide (H_2O_2) and sodium persulfate ($Na_2S_2O_8$). The ability of magnetite (Fe_3O_4) to activate persulfate (PS) and H_2O_2 for the oxidation of IBP at near neutral pH was evaluated as well. The use of soluble Fe^{2+} to activate H_2O_2 and $Na_2S_2O_8$ was also investigated. H_2O_2 and $Na_2S_2O_8$ were inactive during the sixty-minute experiments when used alone. However, activation using Fe^{2+} increased the removal to 95% in the presence of H_2O_2 (Fenton reaction) and 63% in the presence of $Na_2S_2O_8$ at pH 6.6. Chemical oxygen demand (COD) removal was also greater for Fenton oxidation (65%) than for iron-activated PS oxidation (25%). Activation of H_2O_2 and PS by Fe_3O_4 was only observed at a high oxidant concentration and over 48 h of reaction time. A second order rate kinetic constant was determined for H_2O_2 ($3.0*10^{-3}\,M^{-1}\,s^{-1}$) and $Na_2S_2O_8$ ($1.59*10^{-3}\,M^{-1}\,s^{-1}$) in the presence of Fe_3O_4. Finally, several of the degradation products formed during oxidation of IBP in the presence of H_2O_2 and $Na_2S_2O_8$ (activated by Fe^{2+}) were identified. These include oxalic acid, pyruvic acid, formic acid, acetic acid, 4-acetylbenzoic acid, 4-isobutylacetophenone (4-IBAP) and oxo-ibuprofen.

© 2012 Elsevier B.V. All rights reserved.

1. Introduction

Ibuprofen (2-(4-isobutylphenyl) propanoic acid) is a non steroidal anti inflammatory, antipyretic and analgesic drug. It is widely used for the treatment of inflammatory disorders such as rheumatoid arthritis and for pain relief. In 1984 it was approved as an over the counter drug and since then, non-prescription sales have tripled in North America (Caviglioli et al., 2002). IBP is degraded in the human body into its principal metabolites hydroxy-IBP, carboxy-IBP and to carboxy-hydratropic acid (Buser et al., 1999; Fent et al., 2006), which have been found together with IBP in raw sewage (Heberer, 2002). In Canada, IBP and one of its metabolites have been detected in the effluent of a primary wastewater treatment plant at concentrations greater than 500 ng L^{-1} (Gagnon and Lajeunesse, 2008) while in Europe and the US, concentrations of up to 10 µg L^{-1} were detected (Méndez-Arriaga et al., 2010; Pomati et al., 2004; Zorita et al., 2009). There is currently no quantified limit to the discharge of IBP in wastewater from manufacturing plants in Canada. However, considering that some physiological changes such as growth inhibition of a Macrophyte species (Lemna Minor) and stimulated production of the stress hormone abscisic acid in Lemna Minor (Pomati et al., 2004) have been linked to IBP, more stringent regulations are expected in the near future. Simple, efficient and cost-effective treatment options for the

wash-water of vessels used in the production process of IBP-containing pills will thus become essential to the pharmaceutical industry. Various oxidation processes have been investigated for the removal of IBP in water but their efficiencies of removal have varied from no removal to complete removal (Caviglioli et al., 2002; Huber et al., 2003, 2005; Lee and von Gunten, 2009; Madhavan et al., 2010; Méndez-Arriaga et al., 2010, 2008; Skoumal et al., 2009). Furthermore, toxic transformation products were formed in a few cases (Caviglioli et al., 2002; Madhavan et al., 2010; Méndez-Arriaga et al., 2010). More work is thus still needed to identify the best treatment option(s) for IBP-containing industrial wastewaters.

All past research pertaining to the removal of IBP by the Fenton process only considered using soluble Fe^{2+} (traditional Fenton's reagent) and in most of these studies, low pH conditions (pH<4) were required to prevent the precipitation of iron (Méndez-Arriaga et al., 2010; Skoumal et al., 2009). Unlike the classical Fenton process, the reaction of Fe-bearing minerals with hydrogen peroxide (H_2O_2) can effectively improve the oxidation of organic molecules at circumneutral pH. This has been demonstrated for other contaminants such as 2,4,6-trinitrotoluene and phenol (Matta et al., 2007, 2008a, 2008b) but has yet to be shown for IBP. The degradation of pharmaceutical compounds by Fenton's reagent and a Fenton-like system has also been reported at acidic conditions (Goi et al., 2008; Hofmann et al., 2007; Méndez-Arriaga et al., 2010; Skoumal et al., 2009). However the removal of IBP at neutral pH, which is less abrasive to the environment, would be more appealing for applications in the treatment of wastewater or wash water that is produced in IBP processing plants.

* Corresponding author. Tel.: +1 514 398 2273; fax: +1 514 398 6678.
E-mail address: viviane.yargeau@mcgill.ca (V. Yargeau).

Persulfate (PS) was also proven to be very useful for the elimination of contaminants such as diphenylamine, trichloroethylene, benzene, toluene, ethyl benzene and xylene in aqueous and soil slurries (Liang et al., 2004a, 2004b, 2008). However, currently only one study investigated the use of PS or activated-PS for the elimination of a different pharmaceutical product, sulfamonomethoxine (Yan et al., 2010). Although the activation of PS by soluble iron to form a sulfate radical ($SO_4^{\bullet-}$) has been previously reported, the initiation of PS decomposition by iron oxide minerals has been scarcely investigated (Ahmad et al., 2010; Yan et al., 2010).

Minerals like ferrihydrite, goethite, manganese oxide and clay were used to activate the oxidation reaction of organic compounds (Ahmad et al., 2010). Fe^{II}-bearing minerals like magnetite (Fe_3O_4) were found to be the most effective catalyst as compared to the only Fe^{III} oxides for heterogeneous catalytic oxidation of organic pollutants (Ahmad et al., 2010; Matta et al., 2007, 2008b; Xue et al., 2009b, 2009c). In addition, Fe_3O_4 exhibited excellent structural and catalytic stabilities. Fe_3O_4 can be magnetically recovered and reused for several oxidation cycles; it is abundant in environmental settings and has a low solubility in aqueous solution (Schwertmann and Cornell, 2000; Xue et al., 2009a, 2009c). To date, the use of Fe_3O_4 (the most stable mixed valence oxide), to activate PS or H_2O_2, has not been tested for IBP removal.

The objectives of this study were to (i) examine the oxidation of IBP by H_2O_2 and PS at near neutral pH, (ii) test the ability of soluble Fe^{II} and Fe_3O_4 to activate H_2O_2 or PS, (iii) determine the extent of mineralization and identify the degradation products of IBP oxidation.

2. Materials and methods

2.1. Chemicals

Ibuprofen (≥98%), magnetite powder (Fe_3O_4, 98%), sodium persulfate ($Na_2S_2O_8$, 99%), ammonium acetate (≥99.9%) and iron chloride tetrahydrate ($FeCl_{2*}4H_2O$, ≥99%) were purchased from Sigma-Aldrich. Hydrogen peroxide (H_2O_2 35% w/w) was purchased from EMD Chemicals. HPLC grade methanol (≥99.9%) and HPLC grade ammonium acetate (≥99.0%) were purchased from Fisher Scientific. Hydrochloric acid (HCl, >99%), sodium chloride (NaCl, >99.5%), sodium hydroxide (NaOH, 0.1 M), 4-acetylbenzoic acid (98%), oxalic acid (>99%), 4-ethylbenzaldehyde (98%), formic acid (98%), pyruvic acid (98%) and acetic acid (98%) were purchased from Sigma Aldrich. Oxo-ibuprofen was purchased from Santa Cruz Biotechnology Inc., and 4-isobutylacetophenone (4-IBAP, >96%) from TCI America. Nitrogen (N_2, 99.99%) was purchased from Megs.

2.2. Characterization of iron(II, III) oxide

The X-Ray Diffraction (XRD) data were collected with a D8 Bruker diffractometer equipped with a monochromator and a position-sensitive detector to confirm the nature of the oxide (Fe_3O_4) before and after the oxidative treatment. The X-ray source was a Co anode ($\lambda = 0.17902$ nm). The diffractogram was recorded in the 3–64° 2θ range, with a 0.0359° step size and a collecting of 3 s per point. The particle size distribution of Fe_3O_4 was measured using a Mastersizer 2000 from Malvern Instruments. The Tristar 3000 from Quantachrome Instruments was used to determine the specific surface area of Fe_3O_4 by Nitrogen Brunauer–Emmett–Teller (N_2-BET) analysis. The point of zero charge (pzc) of Fe_3O_4 was determined through potentiometric titrations (Xue et al., 2009a).

Scanning Electron Microscopy (SEM) analysis was used to determine the morphology of the purchased Fe_3O_4. The SEM images were collected with a HITACHI FEG 54800 apparatus operated with a beam current of 3 pA and an accelerating voltage of 20 kV (analyzed microvolume of ~6 μm^3). The solid powder was glued on an adhesive surface and metalized with a thin layer of gold.

Transmission Electron Microscopy (TEM) analysis was also performed to obtain information regarding the morphology, the size, shape and arrangement of the particles. TEM observations were carried out with a Philips CM20 TEM (200 kV) coupled with an EDAX energy dispersive X-ray spectrometer (EDXS). The solid powder was re-suspended in 2 mL ethanol under ultrasonication and a drop of suspension was evaporated on a carbon-coated copper grid which was placed on filter paper for analysis.

2.3. Edge sorption and sorption isotherms

Edge sorption experiments were conducted to determine the effect of pH on IBP sorption onto Fe_3O_4. A solution with final concentrations of 0.1 mM IBP and 1 g L^{-1} of Fe_3O_4 ([Fe total] = 13 mM) was prepared in 10 mM NaCl (NaCl was used as the supporting electrolyte). The pH was then adjusted using either HCl or NaOH. For each pH value, 3 mL samples were extracted and filtered through 0.22 μm polyvinylidene fluoride (PVDF) syringe filters (Millipore) that were previously shown not to sorb IBP. A UV–visible spectrophotometer (Agilent 8543 spectrophotometer) was used to determine the IBP concentration in solution at 273 nm and the adsorbed amount was calculated by the depletion method (Matta et al., 2007).

Sorption isotherms were determined at 20 °C. Variable initial IBP concentrations (0–0.5 mM) were prepared with Fe_3O_4 (final concentration of 1 g L^{-1}) at pH 6.6 ± 0.2. As before, the IBP solutions were prepared in 10 mM NaCl. Before analysis, the suspensions were centrifuged, filtered and analyzed by UV–visible spectroscopy as previously described.

2.4. Oxidation experiments

H_2O_2 and $Na_2S_2O_8$ were used to degrade a 0.1 mM solution of IBP (concentration in reverse osmosis water, representative of levels observed in industrial wastewater) in the presence and absence of both Fe^{2+} and Fe_3O_4. Experiments for optimization of oxidant concentration (H_2O_2 and $Na_2S_2O_8$) were first conducted by varying the oxidant concentration between 1 mM and 10 mM in the presence and absence of 1 mM of Fe^{2+}. Replicates were then carried out under the optimal oxidant concentration (in the absence or presence of the iron species) in a 250 mL beaker sealed with parafilm and covered with aluminum foil to prevent any photo-transformation. The experiments were conducted at pH of 6.6 ± 0.2. 3 mL samples were withdrawn at selected time intervals for 60 min and filtered using 0.22 μm syringe filters and analyzed.

For the oxidation experiments using Fe_3O_4, Fe_3O_4 was added at a concentration of 1 g L^{-1} ([Fe total] = 13 mM) before the experiments were initiated. When Fe^{2+} was used, iron chloride tetrahydrate $FeCl_{2*}4H_2O$ was added to the IBP solution to obtain a concentration of 1 mM of Fe^{2+}. N_2 was bubbled in the solution to prevent the oxidation of Fe^{2+} to Fe^{3+} prior to commencing the experiment and throughout.

In order to determine the role of Fe_3O_4 in the kinetic investigation of IBP removal, oxidation experiments were also carried out using higher oxidant concentrations (10 mM) over a longer time frame (48 h).

2.5. Analytical methods

Residual IBP concentration were monitored using High Performance Liquid Chromatography (HPLC) (Agilent Technologies 1200 series) equipped with an Eclipse XDB C-18 (5 μm, 4.6 mm × 250 mm) column (Agilent Technologies) using a diode array detector at a wavelength of 220 nm and 254 nm. Mobile phases consisted of methanol and ammonium acetate (20 mM adjusted to pH 3.0 using formic acid). The flow rate was 0.7 mL/min. The gradient used was the following; 0 min = 60% B, 3% A, 2 min = 67% B, 3% A, 4 min = 74% B, 3% A, 6 min = 81% B, 3% A, 8 min = 88% B, 3% A, 10 min = 95% B, 3% A,

12 min = 97% B, 3% A and 25 min = 97% B, 3% A. Where A is ammonium acetate, B is methanol and the remainder is reverse osmosis water.

The limit of detection of IBP of this method was 0.1 mg L^{-1} (0.5 μM). The product identification was carried out by comparison with standards analyzed using a mass spectrometer (MDS/Sciex QTrap mass spectrometer) equipped with a Turbolon Spray ionization source operated in positive and negative ion mode.

The extent of mineralization was estimated using Chemical Oxygen Demand (COD) measured using a HACH Digital Reactor Block (DRB 200), a HACH spectrophotometer (DR/2500) and low range digestion vials (0–150 mg L^{-1}). Ferrozine method was used to quantify the amount of Fe^{2+} (Kostka and N, 1998; Lovley and P, 1986). Total Fe was determined using Inductively Coupled Plasma Atomic Emission Spectroscopy (ICP-AES) (Thermo Trace Scan equipped with a mini-crossflow nebulizer from SCP Science and a baffled quartz cyclonic spray chamber).

3. Results and discussion

3.1. Characterization of Fe$_3$O$_4$

The XRD diffractogram of Fe$_3$O$_4$ is shown in Fig. 1a. Five diffraction peaks at 2θ = 21.2°, 35°, 41.2°, 50.4° and 62.8° could be assigned to Fe$_3$O$_4$, (Schwertmann and Cornell, 2000). The d-space values of these main peaks were 2.53, 2.96, 2.09, 4.85 and 1.71 Å, which may respectively correspond to the more intense lines of Fe$_3$O$_4$; 311, 220, 400, 111 and 422. Fe$_3$O$_4$ is the only pure oxide of mixed valence and is usually represented by the formula (Fe^{3+})$_{tet}$[Fe^{3+}Fe^{2+}]$_{oct}$O$_4$ (Xue et al., 2009a). It has a cubic spinel structure with iron in both tetrahedral and octahedral sites. The XRD diffractogram recorded at the end of

oxidation reaction was found to be similar to that recorded before reaction, indicating good stability of Fe$_3$O$_4$ during the oxidation process. The surface area determined by BET method was 8.0 m^2 g^{-1}. The pzc value estimated from potentiometric titration was around 9.

SEM image shows that the Fe$_3$O$_4$ particles are highly aggregated and exhibit irregular shapes (Fig. 1b). The size of the particles is non-uniform and ranges between ~100 and ~400 nm. If we consider that the particles are spherical and have a density of 5.15 × 10^6 g m^{-3}, the radius of these particles can be related to the surface area as A = 6/(ρd) = 8 m^2 g^{-1}. Thus, the average diameter calculated assuming a spherical shape is ~150 nm.

TEM image (Fig. 1c) indicates that the Fe$_3$O$_4$ particles are more or less rhombohedral in shape, with crystals varying between 100 and 300 nm in length. TEM combined with EDXS yields an elemental analysis of the sample. Elemental ratios can be calculated by EDXS and compared with known mineralogical compositions. EDX microanalyses of samples before and after oxidation reactions showed the characteristic Fe/O ratio of Fe$_3$O$_4$.

3.2. Sorption of IBP onto Fe$_3$O$_4$

The effect of varying the solution pH value (3–9) on the adsorption of IBP is illustrated in Fig. 2a. Sorption of IBP onto the iron oxide decreases sharply at pH values greater than 5. The observed sorption behavior can be attributed to a combination of pH-dependent speciation of IBP (pK$_a$ = 4.54) and surface charge characteristics of the Fe$_3$O$_4$ (pzc = 9). Based upon surface charging, adsorption is high at low pH values and then decreases when pH increases. The charge repulsion is expected at high pH where the sorbate and sorbent are both negatively charged. Such sorption behavior has also been observed for some
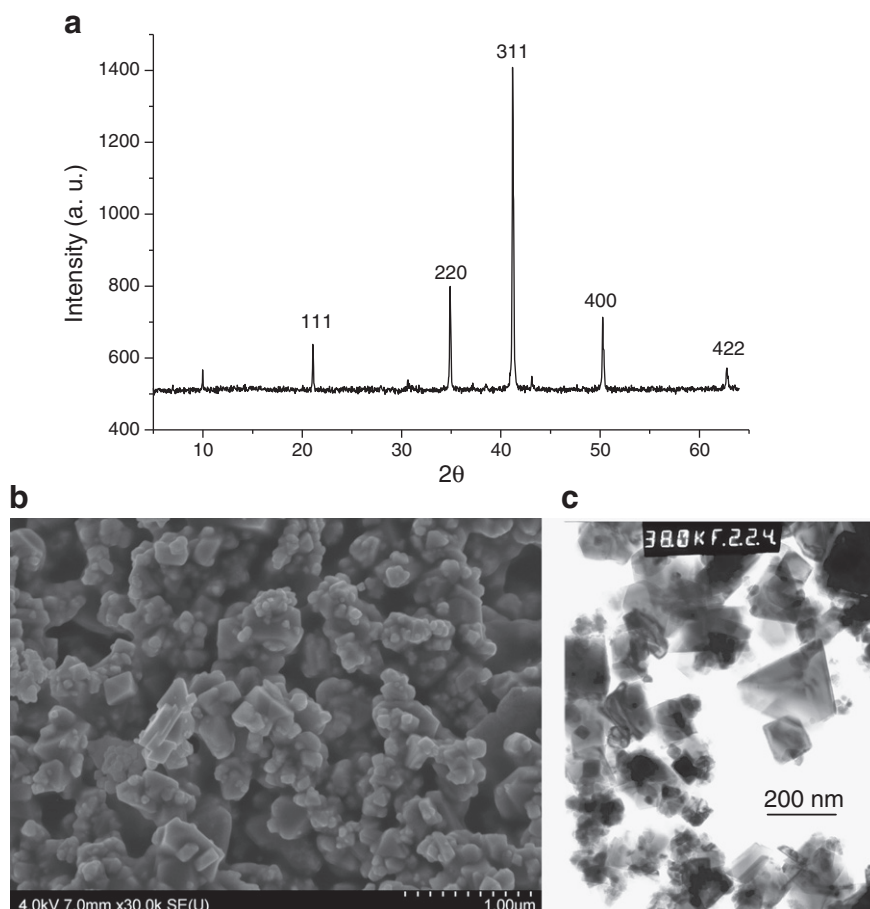

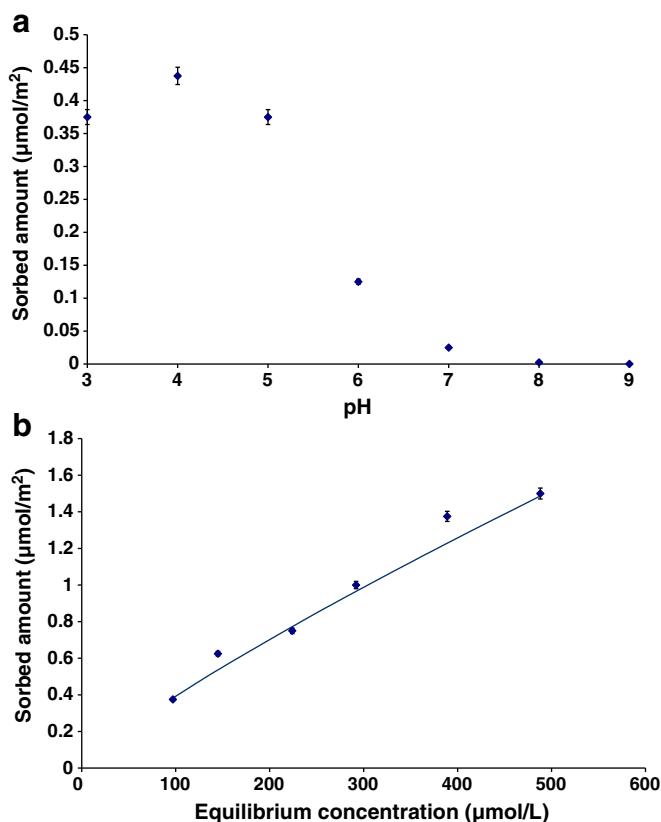**Fig. 1.** (a) XRD diffractogramm (b) SEM and (c) TEM images of the Fe$_3$O$_4$ used.

Fig. 2. (a) IBP sorption onto Fe_3O_4 vs pH. $[Fe_3O_4] = 1$ g/L; [IBP] = 0.1 mM; T = 20 ± 1 °C. (b) Sorption isotherms of IBP onto Fe_3O_4. $[Fe_3O_4] = 1$ g/L; T = 20 ± 1 °C, pH 6.6 ± 0.1; t = 12 h. The line represents the Freundlich model.

organic acid complexation on oxide surfaces (Evanko and Dzombak, 1999). In these studies, the adsorption envelope of monoprotic organic acids bound to iron oxide by surface complexation typically showed maximum adsorption at a pH near their corresponding pK_a.

Sorption isotherms were obtained to evaluate the effect of IBP concentration on sorption to Fe_3O_4 (Fig. 2b). The experimental isotherm data were fitted to the equations of Langmuir and Freundlich by applying linear regression analysis. One way to assess the goodness of fit of experimental isotherm data to these equations is to check the regression coefficients obtained during the regression analysis. On the basis of regression coefficient, the curves were shown a best fit with Freundlich isotherm at the studied range of solute concentration (0–500 μmol/L). The Freundlich equation has been used in the following form:

$$Q = K_F C_e^{1/n} \tag{1}$$

where Q (μmol/m²) is the sorbed concentration, C_e (μmol/L) is the equilibrium concentration at the end of the experiment and K_F and 1/n are Freundlich constants. A plot ($R^2 = 0.98$) of logQ versus logC_e enabled the determination of the Freundlich constants: $K_F = 0.0082$ and 1/n = 0.84.

3.3. Oxidation of IBP

The first objective of the oxidation experiments was to optimize the concentration of H_2O_2 and $Na_2S_2O_8$ in presence of 1 mM of Fe^{2+}. Fe^{2+} concentration was chosen within the range reported in literature for Fenton and PS oxidation ($[Fe^{2+}] = 0.5$ mM −5 mM) (Liang et al., 2004a; Méndez-Arriaga et al., 2010). The optimization of H_2O_2 concentration in the 1 to 10 mM range at pH 6.6 ± 0.2 is illustrated in Fig. 3a. In the absence of iron species, an additional 15% removal was observed

when the concentration of H_2O_2 was increased by 10 fold (from 1 mM to 10 mM). However, in the presence of Fe^{2+}, increasing H_2O_2 concentration had no effect on the removal of IBP. Therefore, the value of 1 mM was chosen for the rest of the experiments.

Optimization experiments for PS oxidation were conducted by varying $Na_2S_2O_8$ concentrations (0.5 mM–2.57 mM) alone and in the presence of a fixed Fe^{2+} concentration (Fig. 3b). Fe^{2+} was set at 1 mM in accordance with literature and more importantly, in order to allow comparison to the Fenton experiments. As illustrated in Fig. 3b, at pH 6.6 ± 0.2 no difference in removal was observed between 1 mM and 2.57 mM of PS. Fe^{2+} content was measured at the end of the experiment using the Ferrozine method. None was detected after 60 min of treatment, indicating that all Fe^{2+} had been completely reacted. Therefore, 1 mM of $Na_2S_2O_8$ or H_2O_2 was selected as optimal concentration for all oxidation experiments.

As shown in Fig. 4a, 1 mM of H_2O_2 used alone or in the presence of Fe_3O_4 led to minimal removal (<1%) over 60 min of reaction time. The oxidation ability of H_2O_2 was strongly enhanced by adding a small quantity of readily available Fe^{2+} which produces Fe^{3+}, hydroxyl radicals (OH•) and hydroxide anions (OH⁻) as demonstrated in previous studies (Méndez-Arriaga et al., 2010; Poyatos et al., 2009; Weiss, 1952). A removal of 95% was obtained after a reaction time of 60 min under these conditions.

Méndez-Arriaga et al. (2010) reported that IBP ($C_o = 0.87$ mM) subjected to varying concentrations of H_2O_2 (8.7×10^{-4} mM–8.7 mM) at a pH and temperature similar to the research presented here resulted in
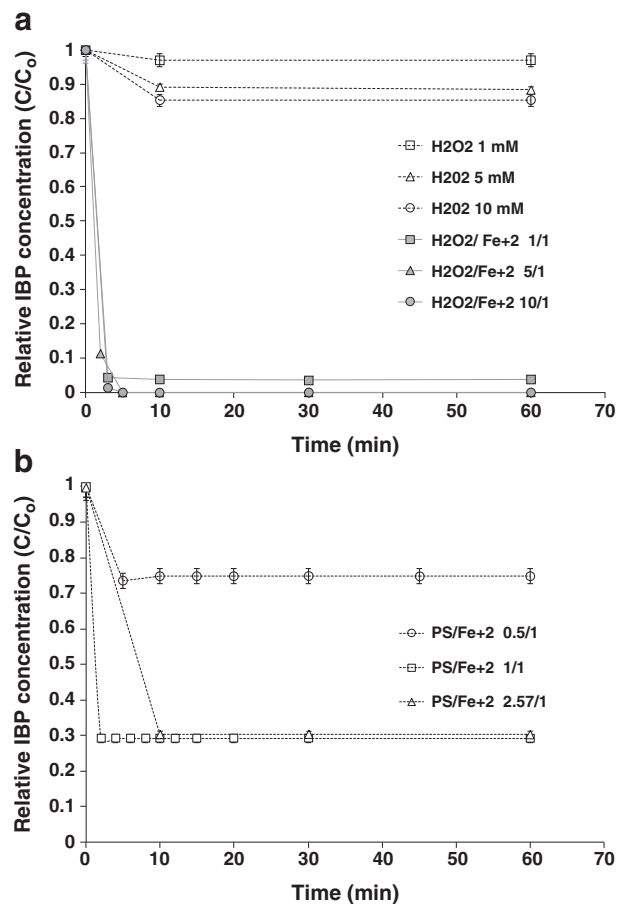

Fig. 3. (a) Removal profile of IBP at various H_2O_2 concentrations $[H_2O_2]$: (□) 1 mM, (△) 5 mM and (o) 10 mM; and in presence of fixed Fe^{2+} concentration $[Fe^{2+}] = 1$ mM, $[H_2O_2]$: (■) 1 mM, (▲) 5 mM and (●) 10 mM. (b) Removal profile of IBP at various PS concentrations in the presence of fixed Fe^{2+} concentration $[Fe^{2+}] = 1$ mM, [PS]: (o) 0.5 mM (□) 1 mM and (△) 2.57 mM. [IBP] = 0.1 mM; T = 20 ± 1 °C.
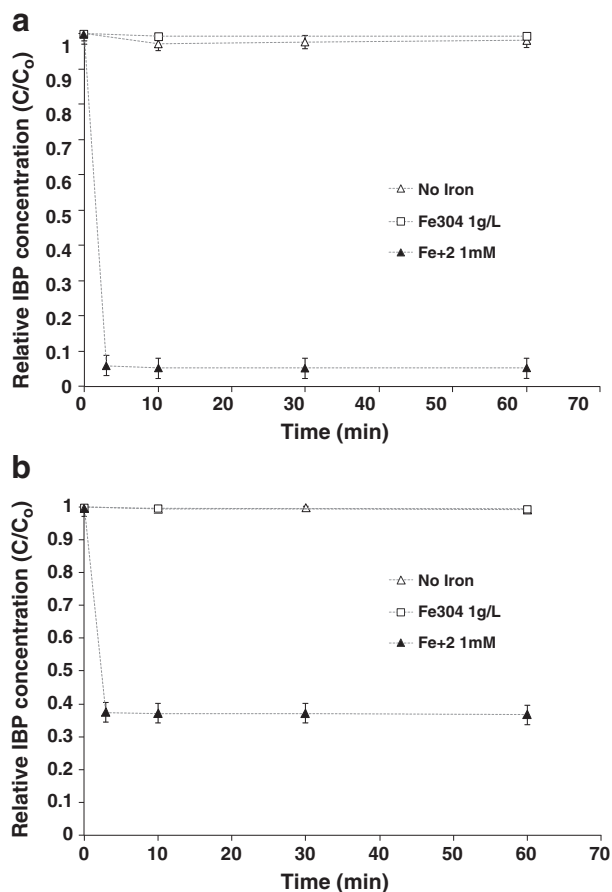
Fig. 4. (a) Oxidation of IBP by H_2O_2 or (b) $Na_2S_2O_8$ in the presence and absence of iron species; (△) absence of iron, (□) $[Fe_3O_4] = 1$ g L^{-1}, (▲) $[Fe^{2+}] = 1$ mM. $[IBP] = 0.1$ mM; $[oxidant] = 1$ mM; $T = 20 \pm 1$ °C.

no removal after 2 h of treatment time. However, they showed that increasing Fe^{2+} concentrations (0.15–1.2 mM) led to higher IBP degradation with an initial H_2O_2 concentration fixed at 0.32 mM. The maximum removal achieved was 60% under the following conditions: $IBP = 0.87$ mM, $Fe^{2+} = 1.2$ mM and $H_2O_2 = 0.32$ mM. This is significantly less than the 95% removal observed in the work presented herein. This could be attributed to two factors: 1) the lower ratio of H_2O_2: Fe^{2+} (1:4) which would lead to a reduced generation of OH• and 2) the higher initial concentration of IBP (~9 times greater than the IBP concentration used in this work) leading to reduced number of oxidizing species per mole of IBP.

During PS oxidation, negligible removal was observed in the absence of iron species and in the presence of Fe_3O_4 while a 63% removal was obtained in presence of Fe^{2+} after 60 min (Fig. 4b). The highly significant impact of adding Fe^{2+} can be explained as follows. The PS anion ($S_2O_8^{2-}$) has a high redox potential ($E^o = 2.01$ V) and is chemically activated by Fe^{2+} to form the sulfate radical ($SO_4^{•-}$), which is an even stronger oxidant ($E^o = 2.4$) (Liang et al., 2004a). $SO_4^{•-}$ can also react with water or OH^- to generate OH• (Peyton, 1993). Furthermore, OH• can initiate a series of propagation reactions that generate perhydroxyl radicals, superoxide radical anions and hydroperoxide anions (Monahan et al., 2005). However, Fe_3O_4 cannot activate PS to form $SO_4^{•-}$ under our experimental conditions (Fig. 4b). Yan et al. (2010) reported that Fe_3O_4 used at a high concentration hindered the PS oxidation of sulfamonomethoxine. In the present work, the high concentration of Fe_3O_4 may have scavenged the $SO_4^{•-}$, leading to the transformation of the radical into the sulfate anion (SO_4^{2-}). This scavenging effect was also observed in previous studies for the heterogeneous Fenton reaction at a high loading of Fe_3O_4 (Xue et al., 2009a, 2009b).

An important observation made during these experiments was that Fe^{2+} quickly oxidized for an almost instantaneous oxidation of IBP; then, the reaction was stalled. This behavior was also observed in the studies of Liang et al. (2004a and 2008) for the PS oxidation of trichloroethylene (TCE) and benzene–toluene–ethylbenzene–xylene (BTEX) compounds. It was hypothesized that this behavior was due to either the destruction of $SO_4^{•-}$ in the presence of excess Fe^{2+} or the rapid conversion of Fe^{2+} to Fe^{3+} (Liang et al., 2004a, 2008). The instantaneous change in color observed when PS was added and the formation of an iron hydroxide precipitate ($Fe(OH)_3$) within the first 3 min strongly suggests that the oxidation of Fe^{2+} was very rapid. In addition, combination of $SO_4^{•-}$ may occur due to an excess of radicals being formed.

Note that kinetic rate constants cannot be determined for the above mentioned oxidation experiments because the removal of IBP in the absence of iron species or presence of Fe_3O_4 was insignificant over the studied reaction time. Furthermore, kinetic investigation was also not considered in the presence of Fe^{2+} due to the rapidity of the reaction, making it impossible to sample over the short reaction time. The following section discusses the kinetic removal of IBP under an extended time frame (48 h) and using a higher initial oxidant concentration in the presence of Fe_3O_4.

3.4. Kinetic of IBP removal using Fe_3O_4

In order to determine the role of Fe_3O_4 on the kinetics of IBP removal, oxidation experiments were carried out using a higher oxidant concentration (10 mM) over a longer time frame (48 h) as proposed in a previous work (Xue et al., 2009a). As illustrated in Fig. 5, the removal of IBP by H_2O_2 alone is minimal (~20%) which is in agreement with previous studies (Méndez-Arriaga et al., 2010; Skoumal et al., 2009). Conversely, H_2O_2 oxidation is significantly enhanced by the presence of Fe_3O_4 (~60%). This behavior was also observed for IBP removal by PS, where the removal was increased from 58% to 73%. The increase in removal for both oxidants is due to the adsorption of IBP onto Fe_3O_4 and to the increased formation of either $SO_4^{•-}$ or OH•. This is a result of using larger initial oxidant concentrations which target the IBP molecule due to the radical's non-selective behavior.

To determine rate constants for Fe_3O_4-activated H_2O_2 and $Na_2S_2O_8$, the raw data was fit to a second order reaction;

$$k * t = \frac{1}{C_a} - \frac{1}{C_{ao}} \qquad (2)$$

where k is the rate order constant (M^{-1} s^{-1}), t is the time (s), C_{ao} is the initial concentration of IBP and C_a (mM) is the remaining concentration of IBP (mM).
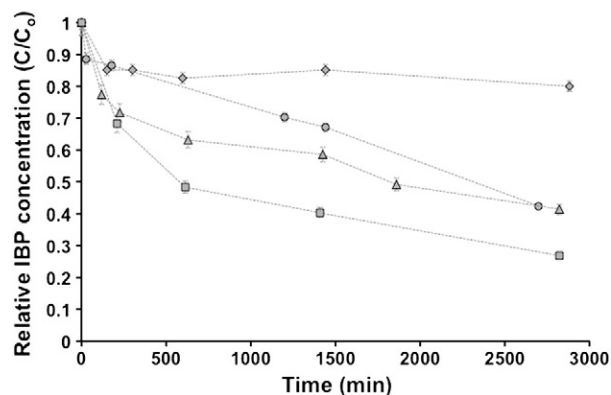

Fig. 5. Oxidation of IBP in the presence of (♦) $[H_2O_2] = 10$ mM, (●) $[Na_2S_2O_8] = 10$ mM, (▲) $[H_2O_2] = 10$ mM + $[Fe_3O_4] = 1$ g L^{-1} and (■) $[Na_2S_2O_8] = 10$ mM + $[Fe_3O_4] = 1$ g L^{-1}. $[IBP] = 0.1$ mM; $T = 20 \pm 1$ °C.

The rate constants for the removal of IBP by the oxidizing species formed were determined to be: $1.59 * 10^{-3} \, M^{-1} \, s^{-1}$ for PS and $3.0 * 10^{-3} \, M^{-1} \, s^{-1}$ for H_2O_2 in the presence of Fe_3O_4. When comparing these results to those obtained by Huber et al. (2003) and Lee and von Gunten (2009), the second order rate constant for the reaction of OH• with IBP($7.4 \times 10^9 \, M^{-1} \, s^{-1}$) is approximately 12 orders of magnitude greater than to $Na_2S_2O_8$ and H_2O_2 in presence of Fe_3O_4. No study has presented the reaction rate constant for IBP removal by $SO_4^{•-}$. In the case of PS and Fenton oxidation, we have seen that Fe_3O_4 can indeed promote the formation of $SO_4^{•-}$ and OH•, however this is hindered if the catalyst loading is too large as these conditions lead to a scavenging effect. Lee and von Gunten (2009) demonstrated that selective oxidants only react with some electron-rich organic moieties, (such as phenols, anilines, olefins, and deprotonated-amine) which are not present in IBP. Therefore the low reaction rate constants can be justified by the scavenging effect of the radicals formed and the non-selective behavior of the oxidants.
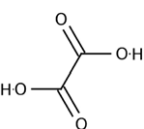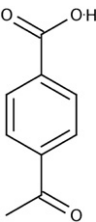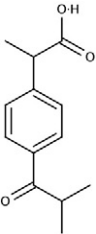
3.5. COD abatement vs. time and identification of degradation products

In order to determine the extent of mineralization, COD was determined in the absence of iron species and in the presence of Fe^{2+} for both oxidants (H_2O_2 or $Na_2S_2O_8$). Fig. 6 presents the average removal obtained with the error bars representing the minimum and maximum values of the replicates. No COD removal was observed for H_2O_2 and PS alone. The addition of Fe^{2+} enhanced the COD removal to 65% and 25% for H_2O_2 and PS, respectively.

Different products were detected as new peaks on the HPLC chromatogram of the samples collected during oxidation with Fe^{2+}. Four of the most abundant degradation products, detected at retention times of 4.6, 4.8, 8.8 and 10.1 min, were collected as fractions. These fractions were analyzed by mass spectrometry (MS) by comparison with standards of compounds reported in literature as potential degradation products of IBP. Table 1 presents these products which were confirmed to be: 4-acetylbenzoic acid, oxalic acid, oxo-ibuprofen and 4-isobutylacetophenone (4-IBAP). 4-IBAP has previously been detected in the environment at the inlet and outlet of a tertiary sewage treatment plant in Sweden (Zorita et al., 2009). Furthermore this product has proven to be quite toxic and the subsequent effects of the compound on the central nervous system are well known (Miranda et al., 1991). No information regarding the persistence or toxicity of 4-acetylbenzoic acid and oxo-ibuprofen has been presented in literature.

Further MS analysis also confirmed the presence of formic acid, pyruvic acid and acetic acid in the treated solution but the presence of 4-ethylbenzaldehyde, also proposed in literature as a potential product, was not confirmed. However, 4-ethylbenzaldehyde is known to have a sweet smell and during the oxidation experiments this type of

Table 1
Degradation products detected by LC and confirmed by MS.

Product	Structure
Oxalic acid	
4-acetylbenzoic acid	
Oxo-ibuprofen	
4-IBAP	
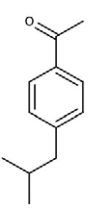
odor was frequently detected and may suggest that this volatile product was formed but did not accumulate in the treated solution. One study determined the lethal dose (LD_{50}) on rats to be 1970 mg kg^{-1} of body weight (Adams et al., 2005). The value presented in literature is not of concern because it is several orders of magnitude higher than what is produced during oxidation. Acetic acid is thought to be formed from pyruvic acid degradation, which has been determined to be a by-product of 4-IBAP. Oxalic acid is mainly formed from the oxidative breakdown of the aryl moiety of aromatics and is largely formed from oxidation of pyruvic and acetic acid. Furthermore, similarly to
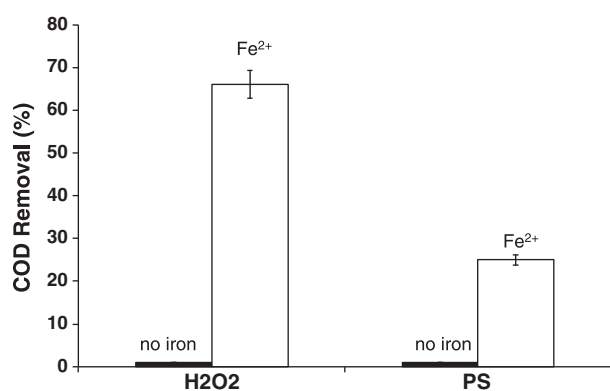

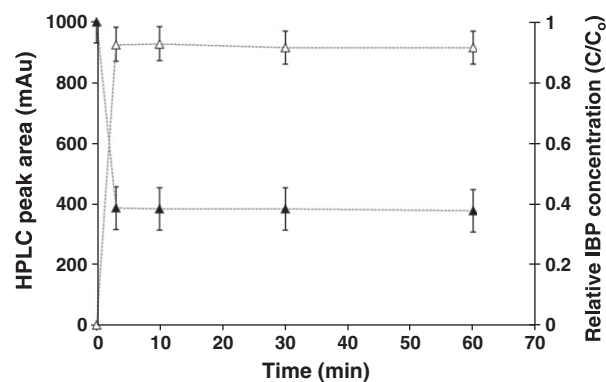**Fig. 6.** COD removal of IBP in the absence of iron species and presence of Fe^{2+}.

Fig. 7. Right axis: removal of IBP with PS activated by Fe^{2+} (▲). Left axis: degradation product formed at retention time 13.2 min during removal of IBP with PS activated by Fe^{2+} (△). [IBP] = 0.1 mM; = 1 mM; T = 20 ± 1 °C; t = 1 h.

oxalic acid, formic acid is an ultimate carboxylic acid since it is directly transformed into CO_2 (Adams et al., 2005; Skoumal et al., 2009).

Due to the low concentration of the degradation products relative to the limit of detection of the HPLC method used, it was not possible to investigate the persistence of the degradation products formed. The peak area of only one degradation product, detected at a retention time of 13.2 min, could be monitored with respect to time. As shown in Fig. 7, this degradation product, which could not be identified by LC-MS, was continuously removed over a period of 30 min even though IBP oxidation had terminated after 3 min during Fe^{2+}-activated PS oxidation. This suggests that there are still oxidizing species present in solution, such as $S_2O_8^{2-}$ which inevitably contributes to the removal of the degradation products.

In the work of Caviglioli et al. (2002), it was noted that several degradation products of IBP form during thermal and oxidative treatments (treatments include; $KMnO_4$, H_2O_2 and $K_2Cr_2O_7$). Only three degradation products detected here were the same as those found in Caviglioli et al. (2002), which were 4-acetylbenzoic acid, oxo-ibuprofen and 4-IBAP. Méndez-Arriaga et al. (2010) reported that hydroxylated byproducts were formed during Fenton treatment and that decarboxylated and hydroxylated byproducts were formed during photo-Fenton treatment (Méndez-Arriaga et al., 2010). Based on the products identified in our study, especially formic acid, which can be formed from decarboxylation of IBP, decarboxylation was thought to be the main mechanism of degradation.

4. Conclusion

The aim of this work was to test the ability of soluble Fe^{2+} and Fe_3O_4 to activate both H_2O_2 and PS. H_2O_2 and $Na_2S_2O_8$ without activation had little effect on IBP removal. When Fe^{2+} was introduced into the system, the removal was greatly enhanced. The removal efficiency increased to 95% in the presence of H_2O_2 and to 63% in the presence of $Na_2S_2O_8$ at pH 6.6. This behavior was also reflected in the COD results.

The Fe_3O_4/H_2O_2 system was also shown for the first time to effectively degrade IBP through a heterogeneous Fenton reaction. The presence of Fe_3O_4 activated PS oxidation of IBP through the possible formation of reactive species such as $SO_4^{\bullet-}$ and $OH\bullet$. A higher kinetic rate constant was found for the oxidation of IBP by H_2O_2 compared to PS in the presence of magnetite. This is the first study to present the reaction rate constant for IBP removal by the $SO_4^{\bullet-}$. Although the kinetics of Fenton-like and PS reactions are slower than those of homogeneous oxidation reactions using Fe^{2+}, the use of Fe_3O_4 as an iron source offers many advantages for engineering application purposes. First, Fe_3O_4 can be used under a wide pH range, unlike homogeneous Fe^{2+} which has a risk of precipitating out at high pH values. Secondly, due to its magnetic properties, Fe_3O_4 particles may be easily separated or recovered from aqueous solutions unlike Fe^{2+} which can form iron sludges. In addition, Fe_3O_4 was shown to be re-usable for further oxidation cycles without attrition and has a low loss of iron content. Furthermore, Fe_3O_4 has a good structural stability during oxidation cycles at neutral pH (Xue et al., 2009a). Therefore it can be hypothesized that re-use would be possible for IBP oxidation as well. The relatively low cost, stability and reusability of Fe_3O_4 make it an environmentally friendly catalyst to remediate an increasing number of environmental pollutants.

Acknowledgments

References

Adams TB, Cohen SM, Doull J, Feron VJ, Goodman JI, Marnett LJ, et al. The FEMA GRAS assessment of benzyl derivatives used as flavor ingredients. Food Chem Toxicol 2005;43:1207–40.

Ahmad M, Teel AL, Watts RJ. Persulfate activation by subsurface minerals. J Contam Hydrol 2010;115:34–45.

Buser H-R, Poiger T, MÄller MD. Occurrence and environmental behavior of the chiral pharmaceutical drug ibuprofen in surface waters and in wastewater. Environ Sci Technol 1999;33:2529–35.

Caviglioli G, Valeria P, Brunella P, Sergio C, Attilia A, Gaetano B. Identification of degradation products of ibuprofen arising from oxidative and thermal treatments. J Pharm Biomed Anal 2002;30:499–509.

Evanko CR, Dzombak DA. Surface complexation modeling of organic acid sorption to goethite. J Colloid Interface Sci 1999;214:189–206.

Fent K, Weston AA, Caminada D. Ecotoxicology of human pharmaceuticals. Aquat Toxicol 2006;76:122–59.

Gagnon C, Lajeunesse A. Persistence and fate of highly soluble pharmaceutical products in various types of municipal waste water treatment plants. Waste Manag Environ IV 2008;109:799–807.

Goi A, Veressinina Y, Trapido M. Degradation of salicylic acid by Fenton and modified Fenton treatment. Chem Eng J 2008;143:1–9.

Heberer T. Occurrence, fate, and removal of pharmaceutical residues in the aquatic environment: a review of recent research data. Toxicol Lett 2002;131:5-17.

Hofmann J, Freier U, Wecks M, Hohmann S. Degradation of diclofenac in water by heterogeneous catalytic oxidation with H_2O_2. Appl Catal Environ 2007;70: 447–51.

Huber MM, Canonica S, Park G-Y, von Gunten U. Oxidation of pharmaceuticals during ozonation and advanced oxidation processes. Environ Sci Technol 2003;37: 1016–24.

Huber MM, Korhonen S, Ternes TA, von Gunten U. Oxidation of pharmaceuticals during water treatment with chlorine dioxide. Water Res 2005;39:3607–17.

Kostka JE, Nealson KH. Chapter 3: isolation, cultivation, and characterization of iron- and manganese-reducing bacteria. New York: Oxford University Press; 1998.

Lee Y, von Gunten U. Oxidative transformation of micropollutants during municipal wastewater treatment: comparison of kinetic aspects of selective (chlorine, chlorine dioxide, ferrateVI, and ozone) and non-selective oxidants (hydroxyl radical). Water Res 2009;44:555–66.

Liang C, Bruell CJ, Marley MC, Sperry KL. Persulfate oxidation for in situ remediation of TCE. I. Activated by ferrous ion with and without a persulfate–thiosulfate redox couple. Chemosphere 2004a;55:1213–23.

Liang C, Bruell CJ, Marley MC, Sperry KL. Persulfate oxidation for in situ remediation of TCE. II. Activated by chelated ferrous ion. Chemosphere 2004b;55: 1225–33.

Liang C, Huang C-F, Chen Y-J. Potential for activated persulfate degradation of BTEX contamination. Water Res 2008;42:4091–100.

Lovley DR, Phillips EJP. Organic matter mineralization with reduction of ferric iron in anaerobic sediments. Appl Environ Microbiol 1986;51:6.

Madhavan J, Grieser F, Ashokkumar M. Combined advanced oxidation processes for the synergistic degradation of ibuprofen in aqueous environments. J Haz Mat 2010;178(1–3):202–8.

Matta R, Hanna K, Chiron S. Fenton-like oxidation of 2,4,6-trinitrotoluene using different iron minerals. Sci Total Environ 2007;385:242–51.

Matta R, Hanna K, Chiron S. Oxidation of phenol by green rust and hydrogen peroxide at neutral pH. Sep Purif Technol 2008a;61:442–6.

Matta R, Hanna K, Kone T, Chiron S. Oxidation of 2,4,6-trinitrotoluene in the presence of different iron-bearing minerals at neutral pH. Chem Eng J 2008b;144:453–8.

Méndez-Arriaga F, Torres-Palma RA, Pétrier C, Esplugas S, Gimenez J, Pulgarin C. Ultrasonic treatment of water contaminated with ibuprofen. Water Res 2008;42: 4243–8.

Méndez-Arriaga F, Esplugas S, Giménez J. Degradation of the emerging contaminant ibuprofen in water by photo-Fenton. Water Res 2010;44:589–95.

Miranda MA, Morera I, Vargas F, Gómez-Lechón MJ, Castell JV. In vitro assessment of the phototoxicity of anti-inflammatory 2-arylpropionic acids. Toxicol Vitro 1991;5: 451–5.

Monahan MJ, Teel AL, Watts RJ. Displacement of five metals sorbed on kaolinite during treatment with modified Fenton's reagent. Water Res 2005;39:2955–63.

Peyton GR. The free-radical chemistry of persulfate-based total organic carbon analyzers. Mar Chem 1993;41:91-103.

Pomati F, Netting AG, Calamari D, Neilan BA. Effects of erythromycin, tetracycline and ibuprofen on the growth of Synechocystis sp. and Lemna minor. Aquat Toxicol 2004;67:387–96.

Poyatos JM, Muñio MM, Almecija MC, Torres JC, Hontoria E, Osorio F. Advanced oxidation processes for wastewater treatment: state of the art. Water Air Soil Pollut 2009.

Schwertmann U, Cornell RM. Magnetite. Iron oxides in the laboratory: preparation and characterization. Weinheim: WILEY-VCH Verlag GmbH; 2000.

Skoumal M, Rodríguez RM, Cabot PL, Centellas F, Garrido JA, Arias C, et al. Electro-Fenton, UVA photoelectro-Fenton and solar photoelectro-Fenton degradation of the drug ibuprofen in acid aqueous medium using platinum and boron-doped diamond anodes. Electrochim Acta 2009;54:2077–85.

Weiss J. The free radical mechanism in the reactions of hydrogen peroxide. In: Frankenburg VIK WG, Rideal EK, editors. Advances in catalysis, Volume 4. Academic Press; 1952. p. 343–65.

Xue X, Hanna K, Abdelmoula M, Deng N. Adsorption and oxidation of PCP on the surface of magnetite: kinetic experiments and spectroscopic investigations. Appl Catal Environ 2009a;89:432–40.

Xue X, Hanna K, Deng N. Fenton-like oxidation of Rhodamine B in the presence of two types of iron(II, III) oxide. J Hazard Mater 2009b;166:407–14.

Xue X, Hanna K, Despas C, Wu F, Deng N. Effect of chelating agent on the oxidation rate of PCP in the magnetite/H_2O_2 system at neutral pH. J Mol Catal A Chem 2009c;311: 29–35.

Yan J, Lei M, Zhu L, Anjum MN, Zou J, Tang H. Degradation of sulfamonomethoxine with Fe_3O_4 magnetic nanoparticles as heterogeneous activator of persulfate. J Hazard Mater 2010;186:1398–404.

Zorita S, Mårtensson L, Mathiasson L. Occurrence and removal of pharmaceuticals in a municipal sewage treatment system in the south of Sweden. Sci Total Environ 2009;407:2760–70.